III-1

Accelerators and Instruments

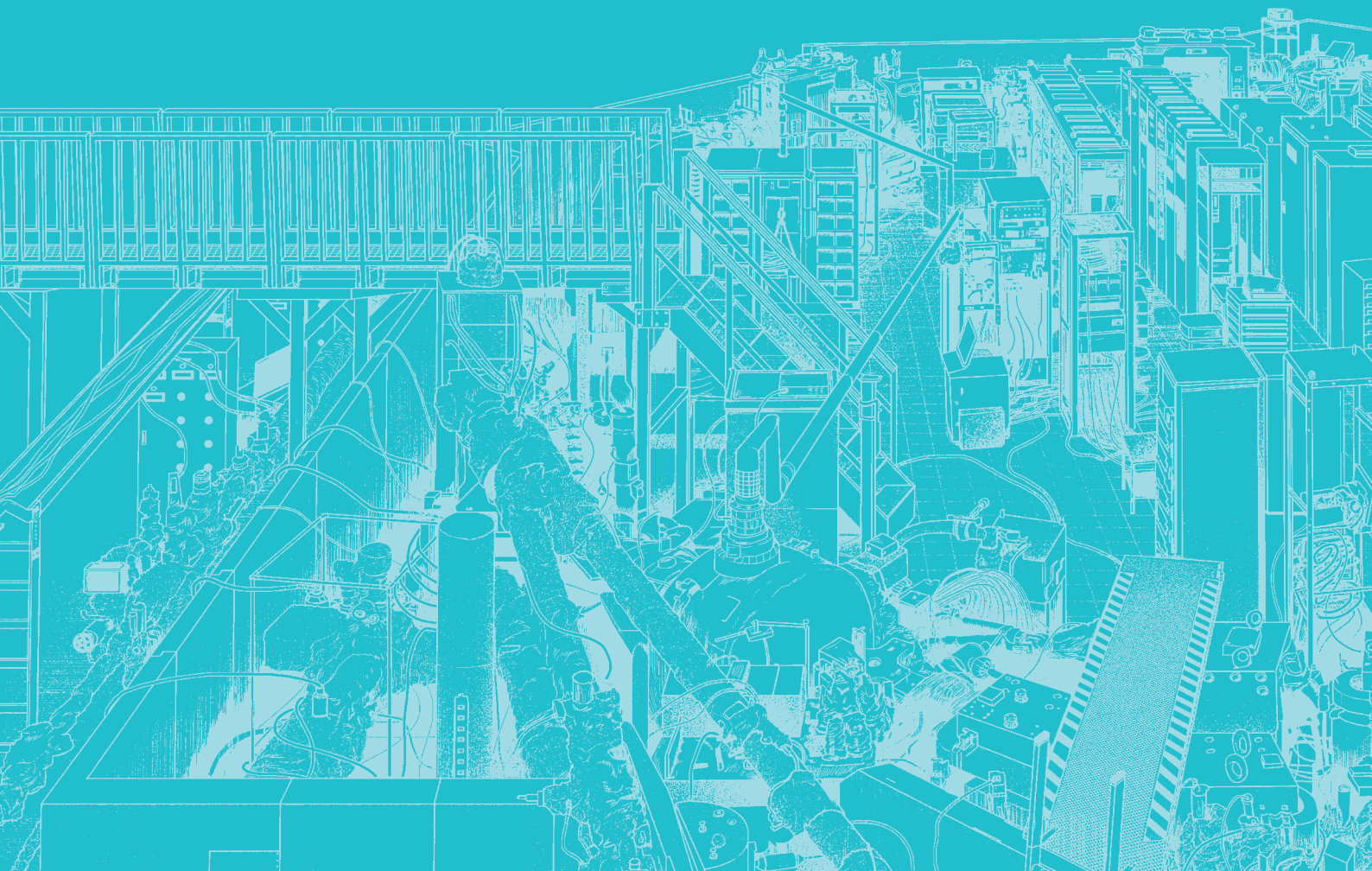

BL1U

Measurements of Temperature-Dependent Absorption Ratios in Transmission Nuclear Resonance Fluorescence

T. Shizuma[1,2], M. Omer[2], R. Hajima[1], M. Koizumi[2], H. Zen[3], H. Ohgaki[3] and Y. Taira[4]

[1]*National Institutes for Quantum Science and Technology, Kizugawa 619-0215, Japan*

[2]*Japan Atomic Energy Agency, Tokai 319-1195, Japan*

[3]*Institute of Advanced energy, Kyoto University, Uji 611-0011, Japan*

[4]*UVSOR Synchrotron Facility, Institute for Molecular Science, Okazaki 444-8585, Japan*

Nuclear Resonance Fluorescence (NRF) is a phenomenon where atomic nuclei absorb and emit γ-rays of specific energies unique to each nuclide. Therefore, by measuring these emitted γ-ray energies, it is possible to identify the nuclide. Additionally, because a γ-ray beam in the MeV energy range is highly penetrating, non-destructive measurement is achievable even when the sample is enclosed in heavy shielding.

In transmission NRF, a γ-ray beam that passes through an absorption target is directed onto another target, called a witness plate (WP), made of the same nuclide as the absorption target. The NRF γ-rays emitted from the WP are then measured. This method is advantageous over scattering NRF as it helps reduce the effects of background radiation [1].

The absorption of γ rays in transmission NRF depends on the temperatures of the absorption and/or WP targets due to variations in the Doppler broadening of the resonant width. As a result, the temperature of the absorption and/or WP targets can affect the measurement's duration and sensitivity. To investigate the temperature dependence of absorption ratios which is defined as $R=1-C/C_0$ where C and C_0 are NRF γ-ray counts with and without the absorption target [2], we irradiated ^{206}Pb samples (both absorption and WP target) at liquid nitrogen (LN_2) temperature using a laser Compton scattering (LCS) γ-ray beam. The LCS γ-rays, with a maximum energy of 5.54 MeV, were produced by the collision of 746-MeV electrons with laser photons of a 1.895 μm wavelength. A 20-cm thick lead collimator with a 3-mm aperture was employed to confine the LCS γ rays, forming the energy width to approximately 8% (FWHM). Two high-purity Ge detectors positioned horizontally at a scattering angle of 90° relative to the incident γ-ray direction were used to measure scattered γ rays from the WP target. The transmitted LCS γ-rays were monitored by a large volume $LaBr_3$ detector placed downstream of the WP target. The experimental setup used for the present measurement is shown in Fig. 1.

Figure 2 shows γ-ray energy spectra measured with (black) and without (red) the absorption target, respectively. Six NRF peaks of ^{206}Pb [3] are observed at 4971, 5037, 5127, 5377, 5470, and 5524 keV. The differences between the intensities at each peak are associated with nuclear resonant absorption (so called self-absorption). The larger the absorption cross section, the greater the difference becomes. The largest self-absorption occurs for the resonance at 5037 keV which has the integrated cross section of 1150 eV b [3]. The measured absorption ratio for this resonance is R=0.68(11) which can be compared with the expected value of 0.58 within the experimental uncertainties. Further analysis is in progress.

This work is in part a contribution of JAEA to IAEA coordinated research program, J02015.

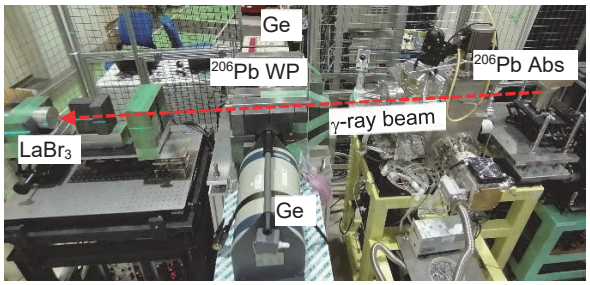

Fig. 1. Photo of the experimental setup used for the present measurement.

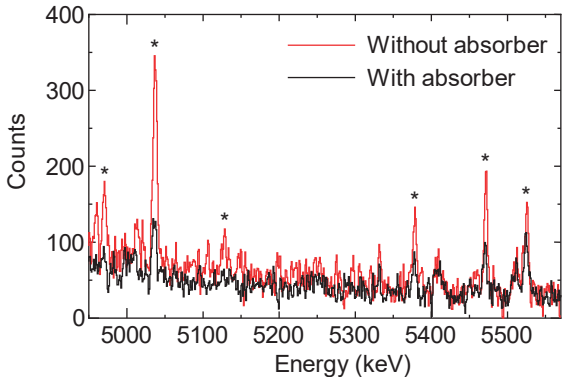

Fig. 2. Energy spectra obtained in transmission NRF experiments. The red (black) spectrum corresponds to the measurement without (with) the absorption target at LN_2 temperature. Asterisks indicate NRF peaks of ^{206}Pb.

[1] C.T. Angell *et al.*, Nucl. Instrum. Methods Phys. Res. B **347** (2006) 11.

[2] F. Metzger, in *Progress in Nuclear Physics*, edited by O. Frisch (Pergamon, New York, 1959), Vol. 7, pp. 53-58.

[3] T. Shizuma *et al.*, Phys. Rev. C **98** (2018) 064317.

Study on 2D Isotope Imaging Using UVSOR-BL1U Undulator

H. Ohgaki[1], K. Nishimoto[1], H. Zen[1], T. Hayakawa[2,3], T. Shizuma[2] and M. Omer[4]

[1]*Institute of Advanced Energy, Kyoto University, Kyoto 611-0011, Japan*

[2]*Kansai Photon Science Institute, National Institutes for Quantum Science and Technology, Kizugawa, Kyoto 619-0215, Japan*

[3]*Institute of Laser Engineering, Osaka University, Suita 565-0871, Japan*

[4]*Integrated Support Center for Nuclear Nonproliferation and Nuclear Security, Japan Atomic Energy Agency, Tokai, Ibaraki 319-1195, Japan*

A flat laser Compton scattering gamma-ray (F-LCS) beam, which has a flat distribution in the energy spectrum and a spatial distribution with a few mm diameter beam size, has been developed to study an isotope selective CT Imaging application at the beamline BL1U in UVSOR[1]. We generate an F-LCS beam by scattering an intense laser beam with a circular-motion electron beam excited by a helical undulator installed at the BL1U beam line. We carried out a proof of principle experiment at the BL1U in UVSOR in 2022 machine time and we obtained a 1D multi-isotope (^{207,208}Pb) imaging using LCS and F-LCS beams in 2023[2].

In 2024, we started evaluation of quantitative information on measured isotopes using an absorption method. We used an absorption target whose composition was one of natural Pb, enriched ^{207}Pb, and ^{208}Pb and three enriched isotope witness targets placed behind the absorption target as shown in Fig.1. The F-LCS beam was generated by using the helical undulator with a K-value of 0.2 as well as normal LCS beam. Most other experimental conditions were the same as the 2023 experiment [2]. To reduce the atomic scattering from the witness targets, the Ge detector angles were changed from 90-deg. in 2023 to 135-deg. We also added the 2nd collimator behind the absorption target to reduce the atomic scattering from the absorption target. The improvement of the background rejection was factor 2 as shown in Fig. 2. Clear NRF peaks from the three witness targets from 5037 keV (^{206}Pb, J^{π}=1$^-$) to 5525 keV (^{206}Pb, J^{π}=1$^-$) were observed. The abundances of ^{207}Pb and ^{208}Pb in the natural Pb target were evaluated by comparison with the NRF yields by the enriched ^{207}Pb and ^{208}Pb targets as the absorption target. The three absorption targets of natural Pb, enriched ^{207}Pb, and ^{208}Pb have the sizes of 5-mm thickness plate, 6.2-mm × 6-mmϕ cylinder, and 15-mm × 8.1-mmϕ (perpendicularly placed). Because the gamma-rays are absorbed by all targets located upstream of the witness target, the thickness correction must be considered for the abundance evaluation. We take into account the atomic absorption in the NRF absorption method, and the result is listed in Table 1[3]. Although the thickness correction to the NRF absorption has not been applied, the evaluated abundances with LCS beams are far beyond the margin of errors. We noticed that the measured $LaBr_3$(Ce) data, which gave the thickness information of the absorption targets, were not reasonable. We are trying to improve the analysis method and figure out the reason for the funny $LaBr_3$(Ce) data.

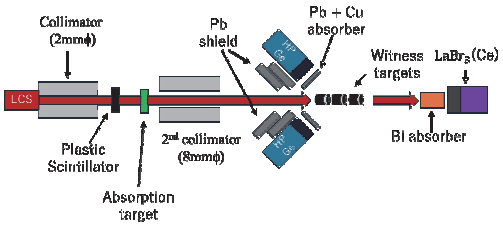

Fig. 1. Schematic drawing of the experiment.

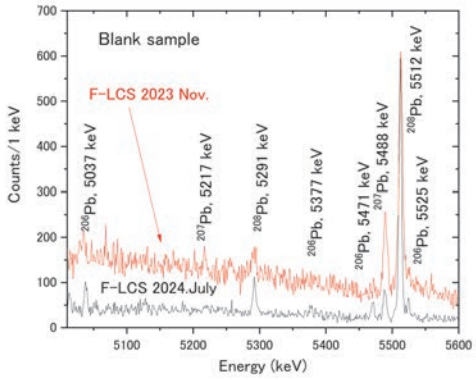

Fig. 2. Measured NRF spectra with the F-LCS beams (red line:2023 Nov., black line: 2024 July).

Table 1. Abundance Evaluation

	Gamma ray beam	^{207}Pb 5488 keV (%)	^{208}Pb 5512 keV (%)
No correction	LCS	−2.9±6.9	46.1±4.2
	F-LCS	11.9±6.2	52.7±5.3
With atomic absorption	LCS	−2.9±6.8	45.7±4.1
	F-LCS	10.6±6.3	52.0±5.3
Established abundance		22.1	52.4

[1] H. Ohgaki *et al.*, Phys. Rev. Accel. Beams **26** (2023) 093402.

[2] H. Ohgaki *et al.*, UVSOR Activity Report **51** (2023) 44.

[3] K. Nishimoto *et al.*, "Quantitative Evaluation of NRF Yield by Using F-LCS beam in UVSOR", AESJ Spring Meeting, online, 2025/03/14.

BL1U

Initial Study of Positron Lifetime Imaging Technique Using Gamma-Ray Beam at UVSOR

S. Takyu[1], Y. Taira[2], T. Hirade[3], F. Nishikido[1], H.G. Kang[1], H. Tashima[1], F. Obata[1], K. Matsumoto[1], M. Takahashi[1] and T. Yamaya[1]

[1]*National Institutes for Quantum Science and Technology (QST), 4-9-1 Anagawa, Inage-ku, Chiba-shi, Chiba 263-8555, Japan*

[2]*National Institutes of Natural Sciences (NINS), 38 NishigoNaka, Myodaiji, Okazaki-shi, Aichi 444-8585, Japan*

[3]*Japan Atomic Energy Agency (JAEA), 2-4 Shirakata, Tokai-mura, Naka-gun, Ibaraki 319-1195, Japan*

Positron emission tomography (PET) is used to diagnose cancer and heart disease, and so on. Unlike CT and MRI, PET can image the internal functions in the living body, and therefore allow us to get closer to the root of internal abnormalities and diseases.

In PET, a positron-emitting drug is administered into the body, and the positrons annihilate with electrons and emit 511 keV photon pairs in the opposite direction, which are detected by a ring-shaped radiation detector. 10^6-10^9 lines of response (LOR) connecting these detection positions are collected, and the drug distribution (radioactivity distribution) is imaged by image reconstruction.

Recently, it has been pointed out that it may be possible to extract new information from the time it takes for positrons to annihilate (lifetime) and use it for diagnosis, because the positron lifetime varies with the surrounding electron density [1]. Therefore, we are currently aiming at the research and development of "quantum PET (Q-PET)" which diagnose by the positron lifetime (Fig. 1.) [2]. To date, we have demonstrated two-dimensional imaging of positron lifetime using a pair of PET detectors [2], and have reported the possibility of imaging hypoxic regions of tumors, which were previously difficult to get quantitative images [3].

However, in living organisms, there are many factors other than oxygen partial pressure that may affect electron density, but there are few basic data that correlates positron lifetime values with diseases. Therefore, the objective of this study is to develop a positron lifetime imaging analysis system that enables three-dimensional analysis of deep inside samples, including living organisms, using 6.6 MeV gamma-ray beam at the UVSOR (Fig. 2. (a)) [4]. Specifically, the beam is irradiated onto the sample, and positrons produced by pair production at the sample depth (to 10 cm) are imaged using the PET principle. The positron lifetime is imaged in three dimensions, with the beam generation as the start and the detection of annihilation photon pairs as the stop. This technique provides accurate information about the start time compared to the technique that accumulates radioisotopes (RIs). This technique also enables three-dimensional analysis of voids in metals and free volume in polymers. This year, we carried out an experiment at UVSOR aimed at the initial demonstration of this technique.

We used one pair of detectors consisting of a 3.2 mm square 8×8 LGSO scintillator array coupled to a 3.2 mm pitch 8×8 MPPC array module. This detector pair was placed opposite each other at a distance of 10 cm, inclined at 15 degrees to the direction of the beam (Fig. 2. (b)). A stainless-steel plate (lifetime value: 106 ps) and a polycarbonate plate (lifetime value: 2.1 ns) were placed separately, and we confirmed the difference in positron lifetime spectra during beam irradiation. We also placed two samples within the field of view of the detector pair and performed simple 2D PET imaging. Details of these achievements will be reported in the conference presentations [5, 6].

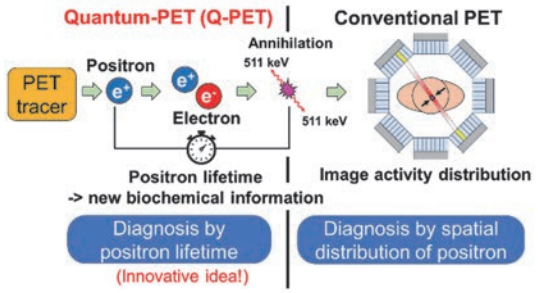

Fig. 1. A difference between quantum PET (Q-PET) and conventional PET.

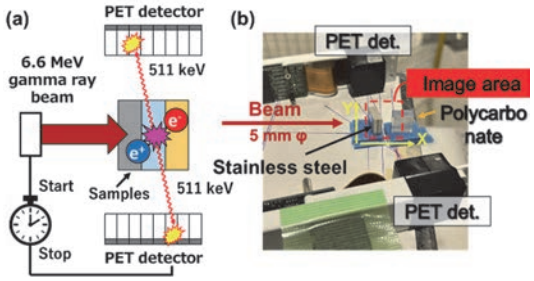

Fig. 2. (a) The principle of the proposed method. (b) The experimental setup.

[1] P. Moskal *et al.,* PET Clin. **15** (2020) 439.
[2] S. Takyu *et al.,* Appl. Phys. Express. **15** (2022) 106001.
[3] S. Takyu *et al.,* Nucl. Instr. Meth. Phys. Res. A. **1065** (2024) 169514.
[4] Y. Taira *et al.,* Rev. Sci. Instrum. **93** (2022) 113304.
[5] S. Takyu *et al.,* Abstract of the 72nd JSAP Spring Meeting 2025, 14p-K502-3, (14, Mach, 2025)
[6] S. Takyu *et al.,* Abstract of the ICPA20, 2025, (submitted)

BL1U

Investigation of Electron Acceleration Location and Condition for Thunderstorm Gamma-ray Flashes

K. Nakazawa[1], A. Tanaka[1], M. Baba[1], Y. Nishimura[1], M. Saito[1], M. Oguchi[1] and K. Okuma[1]
[1]*Graduate school of Sciences, Nagoya University, Nagoya 464-8602, Japan*

Thunderstorm activity is known to produce gamma rays with energies exceeding 30 MeV, which are direct evidence of electron acceleration in the dense atmosphere [1]. Winter thunderstorms along the Sea of Japan is famous for their low-altitude cloud bases (~0.2–0.8 km), which enables ground detection of thunderstorm gamma rays, and we are operating gamma-ray detectors there to understand the location of the acceleration region and its geometry [2-3]. Among them, there are a phenomena called "downward TGFs" which are short duration (< 1 ms), and intense gamma-ray flashes reaching up to 30 MeV [2]. To identify the "origin" of the TGF, we are developing a new detector system, using Cherenkov emission from Compton recoil electron emerged in small acrylic rods, as shown in Fig.1. Our aim is to obtain azimuth and elevation information from the data, and identify the 3D location of the electron acceleration regions, as shown in the right panel of Fig.1.

The detector is made of four acrylic rods, with photo sensors (SiPM) attached to individual ends. As the Cherenkov emission retains some information of the direction of incoming gamma-rays, we can observe the left-right identification of the photon incoming direction by comparing the count rate of the two SiPMs. Although overall performance of the "Cherenkov-rods detectors" have been calibrated using the ~8 MeV gamma-rays from a neutron beam facility KUANS at Kyoto University, the detailed position and angular response of the detector was yet to be understood. We used UVSOR BL1U 6.6 MeV gamma-ray pencil beam and scanned the acrylic rod detector.

We used one acrylic rod for the calibration test in UVSOR. The set up is shown in the left-top panel of Fig.1. Obtained count rates and its ratio as a function of incident angle are summarized in Fig.2. We found that, directed gamma-ray hit to SiPM is non-negligible in side-illumination, while in angled illumination the Cherenkov photon induced events are dominant. The overall angular response is shown in the bottom panel of Fig.2. It reproduced the average profile obtained in the KUANS experiment.

Our experiment in December 2024 was the first time we irradiated a narrow (1 mm) pencil beam to the rod, and found many unexpected, but reasonable phenomena. Based on this result, we are planning more comprehensive experiment to understand the angular response in more detail.

We thank the UVSOR and Dr. Taira for enabling these measurements.

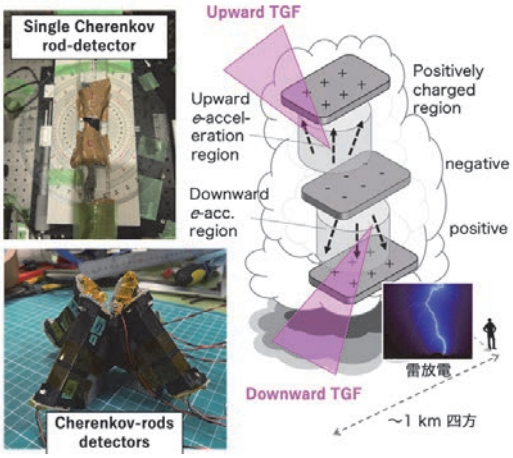

Fig. 1. (right) Concept of our experiment. (left) Our detectors.

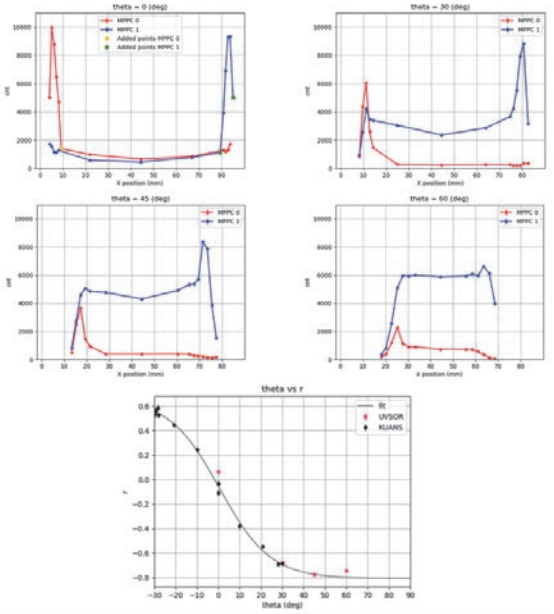

Fig. 2. (top four) Plot of photon count rate vs incident angle. Red is the signals from "right" SiPM and blue is those from "left". (bottom) Angular response as a count-rate ratio as a function of incident angle. UVSOR/BL1U 6.6 MeV result is compared with those obtained in KUANS.

[1] J. R. Dwyer *et al*., Space Sci. Rev. **173** (2012) 133.
[2] T. Enoto *et al*., Nature **551** (2017) 481.
[3] K. Nakazawa *et al*., J. Geophys. Res.:Atmos. **130** (2025) 2024JD042303.

BL1U

Progress in Experimental Study on Single Electron Storage

Y. Asai[1], H. Miyauchi[2, 3], M. Shimada[2, 3] and M. Katoh[2, 4]
[1]*Graduate School of Advanced Science and Engineering, Hiroshima University, Higashi-Hiroshima 739-8526, Japan*
[2]*Research Institute for Synchrotron Radiation Science, Hiroshima University, Higashi-Hiroshima 739-0046, Japan*
[3]*High Energy Accelerator Research Organization (KEK), Tsukuba 305-0801, Japan*
[4]*UVSOR Synchrotron Facility, Institute for Molecular Science, Okazaki 444-8585, Japan*

We have been continuing experimental studies on the single-electron storage at UVSOR-III since 2021 with the aim of conducting fundamental research on the accelerator physics and the electromagnetic radiation from relativistic electrons [1-8]. At BL1U of UVSOR-III, we extracted undulator light in the UV region at a wavelength of 355 nm into the atmosphere through a sapphire window and observed its intensity using a photomultiplier tube with an appropriate band-pass filter to reduce background light. After injecting a small amount of electrons which corresponds to 0.1 mA, the beam current is reduced by using the beam scraper. When the number of the electrons comes to be smaller than a few tens, we observe a step-function-like intensity change with a good SN ratio, that allows us to confirm the number of the stored electrons. When the number of the electrons comes to be unity, we pull out the beam scraper, then the last electron is stored in the ring for longer than several hours.

After establishing the operation technique for the single electron storage described above, we have conducted several experiments, which have been reported elsewhere [3-8]. In this report, we shortly describe a few results from the recent progresses.

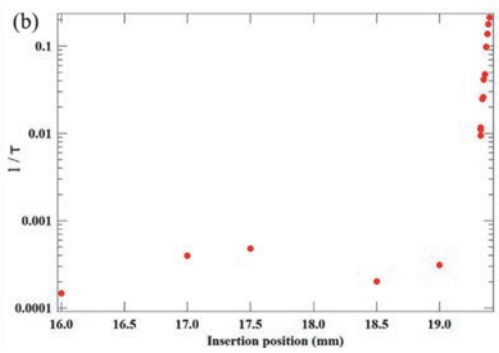

Fig. 1. Beam loss rate vs. Scraper position.

To achieve the single electron storage, we have been using the beam scraper, which is a copper rod installed on the beam pipe. It is inserted to the beam pipe to limit the transverse aperture in the vertical direction. Figure 1 shows the relationship between the insertion position, which is the distance from the pipe wall to the head of the rod, and the beam loss rate. The beam loss rate shows steep increase toward the scraper position around 19.5 mm. The vertical aperture of the beam pipe is 38 mm, which means that the position 19 mm corresponds to the beam center. From the data, the beam center seems to exist at around 19.5 mm. This small discrepancy may arise from the misalignment between the beam and the pipe and also from the mechanical error of the scraper position. When the scraper position is smaller than 19 mm, the beam loss does not show strong dependence on the scraper position. This suggests that, in this range, the beam loss is dominantly caused by the gas scattering or Touschek effect. On the other hand, the beam loss beyond 19 mm is considered to be due to so-called quantum lifetime. Quantitative analysis will be made in near future.

To investigate the properties of radiation from a single electron, we are planning to construct measurement system based on optical fibers, which is expected to make the measurement system more flexible, robust and hard against the background light. We have tested a fiber coupler and a new photomultiplier tube, which is capable of directly producing a photon counting signal without amplifier nor signal processor. The new detector system gave an excellent result in the photon counting measurement.

[1] R. Shinomiya *et al*., UVSOR Activity Report 2021, **40** (2022) 40.
[2] R. Shinomiya *et al*., presented at JSR2022, 9PS01S (Jan., 2022).
[3] Y. Asai *et al*., presented at JSR2023, 1F03S (Jan., 2023).
[4] Y. Asai *et al*., UVSOR Activity Report 2022, **42** (2023) 42.
[5] Y. Asai *et al*., presented at PASJ2023, WEP26 (Aug. 2023).
[6] Y. Asai *et al*., presented at 2023 Annual meeting of JPS, 19aRD11, 3 (Sep., 2023).
[7] Y. Asai *et al*., presented at 2023 HiSOR Symp., P02S (Mar., 2023).
[8] Y. Asai *et al*., presented at 2024 Annual meeting of JPS, 18pB111-11 (Sep., 2024).

BL1U

Spatial Polarization Distribution Measurements of Gamma Rays Produced by Inverse Compton Scattering

Y. Yang[1,3,4], Y. Taira[1,2], T. Shizuma[5] and M. Omer[6]
[1]*Institute for Molecular Science, National Institutes of Natural Sciences, Okazaki 444-8585, Japan*
[2]*School of Physical Sciences, The Graduate University for Advanced Studies (SOKENDAI), Okazaki 444-8585, Japan*
[3]*School of Physics, Zhengzhou university, Zhengzhou 450001, China*
[4]*Shanghai Institute of Applied Physics, Chinese Academy of Sciences, Shanghai 201800, China*
[5]*National Institutes for Quantum Science and Technology, Kizugawa 619-0215, Japan*
[6]*Integrated Support Center for Nuclear Nonproliferation and Nuclear Security, Japan Atomic Energy Agency, Tokai 319-1195, Japan*
Email:yangyuxuan@ims.ac.jp

Polarization measurements of MeV gamma-rays are essential in astrophysics and nuclear physics, offering profound insights into fundamental physical processes [1]. Highly polarized MeV gamma rays can be generated in the laboratory by inverse Compton scattering (ICS) of a polarized laser with a relativistic electron beam. ICS gamma rays possess characteristics such as energy tunable, quasi-monochromatic, and a low divergence angle (<1 mrad). At the UVSOR synchrotron facility, 6.6 MeV gamma rays can be generated by a 90° collisional ICS between a 750 MeV electron beam and an 800 nm laser. The gamma rays are used for user applications such as positron annihilation spectroscopy and detector evaluation of polarized gamma-ray detectors.

By shifting the position of the lead collimator, which is placed on the gamma-ray beam axis, the gamma-ray energy can be changed in the range of 3 ~ 6.6 MeV [2]. However, since the polarization of ICS gamma rays also varies with the position of the beam cross-section, it is necessary to measure the two-dimensional polarization distribution of the gamma rays. We have developed a new polarimeter that can measure the linear polarization of gamma rays in the MeV region. The measurement setup is shown in Fig. 1. The system enables asymmetry analysis of Compton scattering cross-sections using a 50-mm-thick iron target and seven NaI detectors arranged at the scattering angle of 45° with the azimuthal angles spanning 0°~180° in 30° increments. Figure 2 shows the azimuthal distribution of Compton scattered gamma rays when vertically polarized gamma rays are measured, allowing us to measure the asymmetry due to polarization.

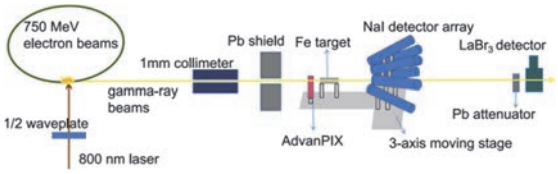

Fig. 1. The Schematic illustration of the spatial polarization distribution measurement.

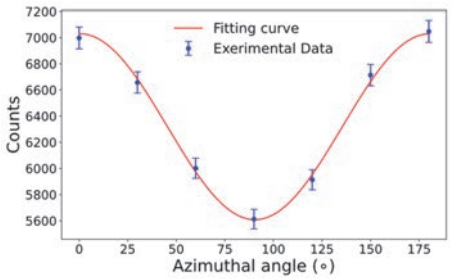

Fig. 2. Azimuthal scattering distribution of vertically polarized gamma-rays when collimator position is horizontal $x = 0$ mm and vertical $y = 4$ mm.

The ICS gamma-ray beam was collimated by a 1-mm lead collimator and then irradiated to the iron target. Two dimensional spatial polarization distribution of ICS gamma rays can be obtained by measuring the azimuthal distribution of Compton scattered gamma rays while shifiting the collimator, target, and detectors in two dimensions. Simultaneously, the gamma-ray beam profile injecting into the target was monitored using an AdvanPIX CdTe image sensor, and the ICS gamma energy spectrum was recorded by a $LaBr_3$ detector. The range of the two dimensional scan was $0 \leq \gamma\theta \leq 1$ and $0 \leq \phi \leq 2\pi$, which sufficiently covers the cross section of the ICS gamma-ray beam, where γ is the Lorentz factor of the electron beam, θ is the scattering angle of gamma rays, and ϕ is the azimuthal angle.

We measured the two-dimensional spatial polarization distribution of horizontally and vertically linearly polarized gamma rays. Building on this methodology, the two-dimensional polarization distributions of ICS gamma rays generated by using a radially and azimuthally polarized laser [3] will be evaluated.

[1] J. Speth *et.al.*, Rep. Prog. Phys. **44** (1981) 719.
[2] Y. Taira *et.al.*, Phys. Rev. A **107** (2023) 063503.
[3] Y. Taira, Phys. Rev. A **110** (2024) 043525.

BL2A

Success of the World's First Solar Flare X-ray Focusing Imaging Spectroscopic Observation by the Sounding Rocket Experiment FOXSI-4 and Post-Flight Calibration of Its CMOS Sensors

N. Narukage [1,2], T. Hirose[1,2], Y. Sato[2,1] and R. Shimizu[2,3]

[1]*National Astronomical Observatory of Japan (NAOJ), Mitaka 181-8588, Japan*

[2]*The Graduate University for Advanced Studies, SOKENDAI, Hayama 240-0193, Japan*

[3]*Institute of Space and Astronautical Science (ISAS), Japan Aerospace Exploration Agency (JAXA), Sagamihara 252-5210, Japan*

The solar corona is full of dynamic phenomena such as solar flares. The understanding of these phenomena has progressed step-by-step with the evolution of observation technology in EUV and X-rays from space. But fundamental questions remain unanswered or have not been addressed so far. Our scientific objective is to understand the underlying physics of the dynamic phenomena in the solar corona, covering some of the long-standing questions in solar physics, such as particle acceleration in flares and coronal heating. To achieve this objective, we identify imaging spectroscopy (the observations with spatial, temporal, and energy resolutions) in the soft X-ray range (from ~0.5 keV to ~10 keV) as a powerful approach for the detection and analysis of energetic events [1]. This energy range contains many lines emitted below 1 MK to beyond 10 MK plasmas and a continuum component reflecting the electron temperature.

The soft X-ray imaging spectroscopy is realized with the following method. We take images with a short enough exposure to detect only single X-ray photon in an isolated pixel area with a fine pixel Silicon sensor. So, we can measure the energy of the X-ray photons one by one with spatial and temporal resolutions. When we use a high-speed soft X-ray camera that can perform the continuous exposure with a rate of more than several hundred times per second, we can count the photon energy with a rate of several 10 photons/pixel/second. This high-speed exposure is enough to track the time evolution of spectra generated by dynamic phenomena in the solar corona including solar flares, whose lifetimes are about from several ten seconds to several ten minutes.

For the world's first focusing imaging-spectroscopic observation of a solar flare in X-ray range, we launched a NASA's sounding rocket as the fourth flight of FOXSI sounding rocket series (called "FOXSI-4") on April 17th, 2024 (Fig. 1) and successfully obtained the unprecedented solar flare data using a combination of high-precision X-ray mirrors and high-speed X-ray cameras (Fig. 2). For the soft X-ray cameras, we use fully depleted CMOS sensors with a silicon thickness of 25 μm [2,3], which provide high sensitivity to high-energy X-rays.

FOXSI-4 detected more than 10^7 X-ray photons during an observation period of about 5 minutes. Using these photons, we can make spatially and temporally resolved X-ray spectra from a solar flare (see Fig. 3) and then investigate the physics of the high-energy plasmas generated by the solar flare.

For the precise scientific analysis of FOXSI-4 data, post-flight calibration of the CMOS sensors is indispensable. In FY2024, this was done for the energy range from 0.85 keV to 4.5 keV at UVSOR BL2A.

Fig. 1. Photo of FOXSI-4 launch at Poker Flat Research Range in Alaska.

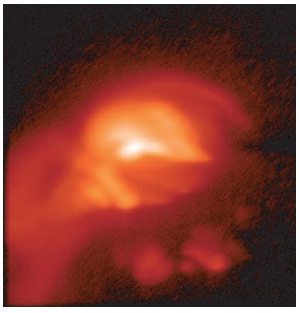

Fig. 2. A solar flare image in soft X-rays observed by the CMOS camera aboard FOXSI-4 sounding rocket.

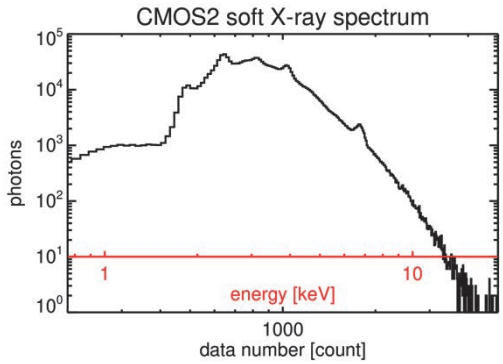

Fig. 3. A soft X-ray spectrum of a solar flare obtained with the CMOS camera aboard FOXSI-4.

[1] N. Narukage *et al.*, White paper of the "soft X-ray imaging spectroscopy", arXiv:1706.04536 (2017).
[2] N. Narukage *et al.*, UVSOR Activity Report **51** (2023) 48.
[3] R. Shimizu *et al.*, Proc. SPIE Int. Soc. Opt. Eng. **13103** (2024) 1310308.

BL2A

Operando Analysis of Battery Materials Using NEXAFS Spectroscopy with a Transportable Potential-Applying Manipulator

E. Kobayashi[1] and A. Inoishi[2]
[1]*Kyushu Synchrotron Light Research Center, 8-7 Yayoigaoka, Tosu, Saga 841-0005, Japan*
[2]*Institute for Materials Chemistry and Engineering, Kyushu University*
6-1 Kasuga-koen, Kasuga-Shi 816-8580, Japan

III-1

Research on battery materials is actively being conducted from the perspective of resource and energy issues, as well as global environmental concerns. In the development of new battery materials, information on changes in the valence of each element before and after the application of potential to the fabricated battery is essential for analyzing the reaction mechanism. Moreover, operando measurements during analysis enable more accurate reaction analysis. Additionally, in the analysis of battery materials, non-exposure measurements to atmospheric components are indispensable due to the materials' reactivity to atmospheric substances. From this perspective, we developed a manipulator for soft X-ray absorption spectroscopy that allows samples to be transported without exposure to the atmosphere [1].

The elements contained in battery materials exhibit a wide range of absorption edge energies, from lithium to sulfur, chlorine, and even metals. Consequently, depending on the synchrotron radiation facility, it may not be possible to measure all elements on a same beamline, or the facility itself might not be able to accommodate the measurements. Furthermore, due to differences in sample holders across facilities and beamlines, challenges arise when handling rare samples, such as difficulty in making adjustments and reproducing surface conditions. To enable analysis of the surface state of the same sample, we developed a transportable manipulator [1]. This device allows the sample to be directly attached to the sample-fixing part and transported under vacuum or gas atmospheres. The sample-fixing part is connected to a coaxial feedthrough Bayonet Neill-Concelman (BNC) at the top of the device, enabling the measurement of sample current. Furthermore, since the device can be installed on the conflat flange with an outer diameter of 70 mm (ICF70) port, it facilitates cross-beamline or cross-facility measurements. Additionally, to more accurately evaluate the reactions occurring in batteries, we developed a device capable of applying voltage to the battery, allowing for measurements of the actual reaction state under operational conditions [2].

Previously, the soft X-ray absorption spectra of electrodes and solid electrolytes were measured after disassembling batteries that had undergone charge and discharge cycles without exposure to the atmosphere. However, since the samples used were different, the changes due to charge and discharge were not fully reflected. On the other hand, operando observation allows for the monitoring of changes at the same location, which is expected to enable a more accurate evaluation of electrochemical changes. In this study, we analyze battery materials using a manipulator capable of applying voltage.

The sample was attached to the transfer vessel in a glove box under an argon atmosphere and transported to the analyzer. Soft X-ray absorption spectrum of the sample was measured at the BL2A of the UVSOR in the Institute for Molecular Science. The XAFS spectra was obtained using the partial fluorescence yield (PFY) mode at room temperature. Fluorescence detector used was a silicon drift detector (SDD).

Figure 1 shows the time dependence results of the Mg K-edge NEXAFS of MgI_2 under applied voltage. The peak near 1305 eV, which corresponds to metallic Mg, was not observed. This is because the battery had high resistance and not enough electricity flowed, so the electrode reaction did not progress to a detectable range. However, as discharge progressed, the spectrum shifted slightly to the lower energy side. This indicates that the slight changes associated with the reduction reaction at the electrode could be observed using this device.

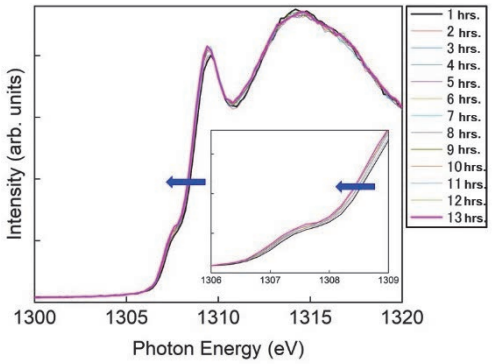

Fig. 1. Mg K-edge NEXAFS of MgI_2 under applied voltage.

[1] E. Kobayashi and A. Inoishi, UVSOR Activity Report **50** (2022) 44.
[2] E. Kobayashi and A. Inoishi, UVSOR Activity Report **51** (2023) 49.

BL3B

Low Temperature Measurements to Understand Luminescence Characteristics of Synthetic Diamond

Atsuhiro Umemoto[1]

[1]*International Center for Quantum-field Measurement Systems for Studies of the Universe and Particles (QUP), High Energy Accelerator Research Organization (KEK), Tsukuba 305-0801, Japan*

Diamond is a wide-bandgap semiconductor with unique physical properties, such as the highest Debye temperature among crystals and easy formation of optical color centers by impurity doping. Owing to these characteristics, diamond is expected to be used as a scintillating bolometer in the field of particle physics, detecting both luminescence and heat generated by charged particles. Scintillating bolometers exhibit excellent energy resolution and particle identification capabilities, which are important for rare event searches, such as dark matter search. We have been conducting research and development on both diamond scintillators and bolometers for dark matter detection. Recently, we have shown the basic characteristics of diamond scintillators by using nitrogen-doped, commercially available synthetic crystals [1]. At present, with the cooperation of Prof. Taniguchi and Miyakawa at the Research Center for Materials Nano-Architectonics, National Institute for Materials Science, synthetic diamonds with controlled dopants for optical color centers can be manufactured and used to study their luminescence properties.

During the beam time in FY2024, photoluminescence measurements were conducted on synthetic diamonds with nitrogen concentrations ranging from 1 to 200 ppm. Since scintillating bolometers operate at low temperatures, understanding their luminescence characteristics at these temperatures is very important. Figure 1 shows a comparison of the photoluminescence spectra of diamond with a nitrogen concentration of 1 ppm, measured at different temperatures. The excitation wavelength was set to λ=220 nm, which is a similar energy as the bandgap of diamond. The peak wavelength shifted from 516 nm to 569 nm when the temperature was lowered from room temperature to 7 K. While a detailed analysis has not yet been conducted, this suggests that lowering the temperature may have induced changes in the crystal structure. In any case, luminescence was observed at low temperatures, and although it was not easy to quantify the light yield, it was shown to be comparable to that at room temperature. As an interesting point from physical properties perspective, we observed that the change in the peak wavelength between low and room temperatures depends on the nitrogen concentration. The linear line shown in Fig. 2 represents predictions, but the peak wavelength might shift to shorter wavelengths at lower temperatures when the nitrogen impurity concentration exceeds 150 ppm.

The decay time constants of luminescence and other parameters show different behavior in samples with nitrogen impurity concentrations exceeding 150 ppm. Further investigations are needed to understand the luminescence characteristics at low temperatures and to determine the optimal nitrogen concentration for dark matter search.

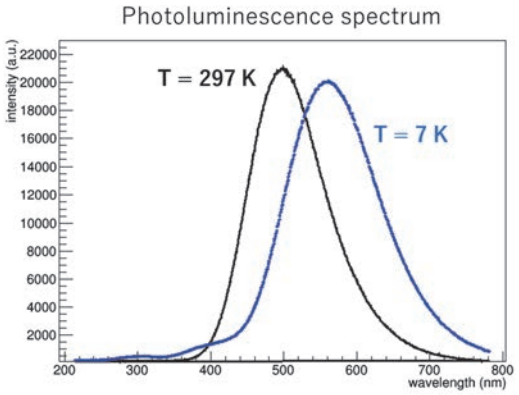

Fig. 1. Photoluminescence spectra of nitrogen-doped synthetic diamond with a nitrogen concentration of 1 ppm, measured at different sample temperatures.

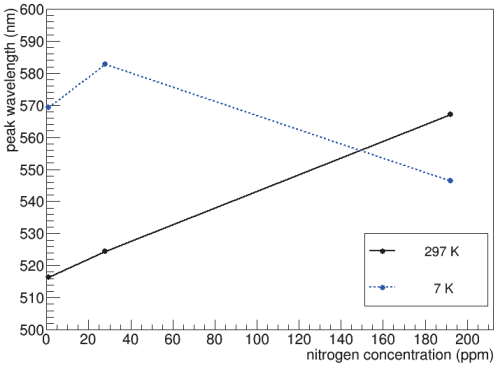

Fig. 2. The shift of the photoluminescence peak wavelength depended on the temperature. It was performed on three samples with different nitrogen concentrations.

[1] A. Umemoto *et al*., Nucl. Instrum. Methods A **1057** (2023) 168789.

Development of a Lyman-α Detector

T. Kaneyasu[1,2] and M. Kobayashi[3]
[1]*SAGA Light Source, Tosu 841-0005, Japan*
[2]*UVSOR Synchrotron Facility, Institute for Molecular Science, Okazaki 444-8585, Japan*
[3]*National Institute for Fusion Science, Toki 509-5292, Japan*

The attosecond phase-control of electromagnetic radiation from an ultra-relativistic electron is a new capability of synchrotron radiation that allows the control of quantum wave packet interference in the short wavelength regime [1,2]. This unmarked capability of synchrotron radiation has been successfully applied to quantum control and ultrafast spectroscopy of atoms in the extreme ultraviolet wavelength. As a next step of the quantum control by synchrotron radiation, we plan to observe the quantum interference between the vibrational wave packets in the hydrogen molecule excited by vacuum ultraviolet (VUV) pulses.

In the designed experiment, the hydrogen molecule interacts with a pair of VUV pulses. The quantum interference between the vibrational wave packets is monitored by detecting the fluorescence in the ultraviolet wavelength. In particular, the Lyman-α emission from a fragment can be used to probe the vibrational excitation in a particular state [3].

Figure 1 shows the developed detector. The Lyman-α detector consists of a gas cell and a micro-channel plate (MCP). The gas cell is equipped with a MgF_2 window which allows selective detection of fluorescence larger than 120 nm wavelength. The MCP is coated with CsI to increase the quantum efficiency in the VUV wavelength.

As a performance test of the detector system, we have measured the fluorescence yield spectrum of hydrogen molecules in the VUV wavelength at BL7B. The detection angle was set to be 55 degrees with respect to the polarization vector of the synchrotron radiation. A Nb filter of 160 nm thickness was inserted in front of the experimental chamber to filter out the second harmonic and to maintain the ultrahigh vacuum condition in the beamline.

Figure 2 shows the fluorescence yield spectrum where we have assigned three vibrational progressions belonging to the B $^1\Sigma_u^+$, C $^1\Pi_u$, and D $^1\Pi_u$ electronic states according to the EELS study [4]. The Lyman-α from the D state is attributed to the production of H(2*l*) atoms generated by the predissociation of the vibrationally excited states. In contrast to the spectrum measured with a detector equipped with a ceratron [3], the fluorescence yield from the B and C states is enhanced in the observed spectrum. They are most likely a consequence of the molecular fluorescence of more than 150 nm wavelength emitted from these states [5]. Given that the relative quantum efficiency of the CsI-coated MCP for the 150 nm wavelength is about one order of magnitude higher than that for the Lyman-α wavelength [6], the fluorescence intensity is enhanced in the region of the B and C states. The performance of the detector is satisfactory, and its application to the quantum interference experiment is planned.

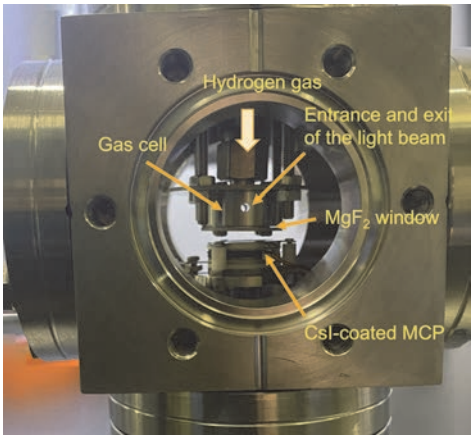

Fig. 1. Photo of the Lyman-α detector. The detector components were assembled inside the ICF-70 cube-type chamber.

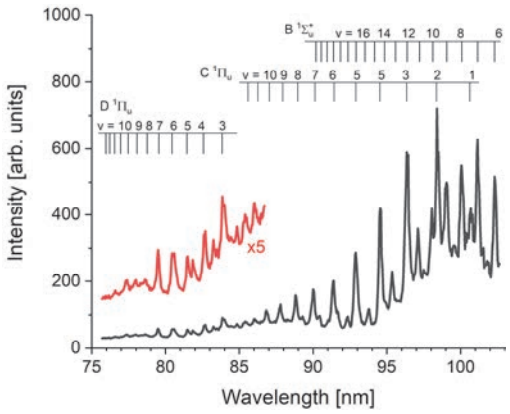

Fig. 2. VUV fluorescence yield spectrum measured by the Lyman-α detector.

[1] Y. Hikosaka *et al.*, Nat. Commun. **10** (2019) 4988.
[2] T. Kaneyasu *et al.*, Phys. Rev. Lett. **126** (2021) 113202.
[3] S. Arai *et al.*, Z. Phys. D **4** (1986) 65.
[4] W. F. Chan *et al.*, Chem. Phys. **168** (1992) 375.
[5] P. Schmidt *et al.*, J. Phys. Conf. Ser. **635** (2015) 112130.
[6] Kuwabara *et al.*, JAXA-RR-16-011 (2017).

Others

Development of Nuclear Emulsion Focusing on Gelatin Composition for Suppression of Latent Image Fading

A. Yoshihara[1], K. Morishima[1], N. Kitagawa[1] and T. Yoshida[1]
[1]*Graduate School of Science, Nagoya University, Nagoya 464-8602, Japan*

Nuclear emulsion is three-dimensional radiation detector consisting of emulsion in which AgBr crystals are dispersed in gelatin and coated onto a support. When a charged particle passes through the emulsion layer, ionization generates electrons. These electrons combine with silver ions to form latent image (Ag_n) consisting of multiple silver atoms. In development process, only latent image with n≥4 is developed and recorded as tracks.

Nuclear emulsion is being used in various fields, one notable example being Cosmic ray imaging. Cosmic ray imaging is new non-destructive inspection technique of large-scale constructions with cosmic ray muon. We had ever applied this technique to the pyramid of khufu in Egypt and discovered a big void [1]. To further expand its application to diverse structures, improving detector's temperature resistance is essential.

The issue of temperature resistance is latent image fading. Latent image fading refers to the gradual disappearance of tracks under high-temperature conditions. One possible cause is the oxidation of latent image by Br_2, which reduces their size and makes them undevelopable [2]. As shown in Fig 1, GD [counts/100μm] decreases over time in high-temperature conditions.

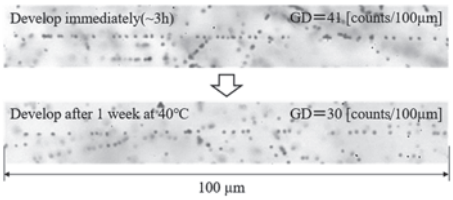

Fig.1. Latent image fading of electron tracks irradiated at UVSOR.

To suppress of latent image fading, we propose a method to prevent Br_2 from approaching the latent image. Specifically, we utilize halogen bonding with sulfur compounds in gelatin to capture and immobilize Br_2. Typically, bovine bone gelatin used in nuclear emulsions contains only methionine as sulfur compound, with approximately four functional groups per 10^3 Amino acids. To increase the amount of sulfur compounds in gelatin, we developed "thiol-introduced gelatin" by artificially incorporating sulfur compounds. Additionally, we used "fish gelatin" which naturally contains the highest amount of sulfur compounds among natural sources, to produce nuclear emulsions. Table 1 shows the sulfur compound content of each gelatin type. Since neither type of gelatin has been previously applied to nuclear emulsions, evaluation is essential.

Table 1. Amount of functional groups with sulfur in each gelatin [/10^3 Amino acids]

	Bovine bone gel	Thiol gel	Fish gel
Methionine	4	4	10
Thiol	-	4	-
Total	4	10	10

As a result of its application, thiol-introduced gelatin was confirmed to form a strong bond between Ag^+ on the AgBr surface and thiol groups, leading to the coagulation of the emulsion. We prevented coagulation by adding NaBr solution, making its application feasible. In case of fish gelatin, due to its low molecular weight and low viscosity, preventing it from adequately supporting AgBr, which resulted in sedimentation. We introduced thickening agents to crosslink gelatin molecules, increasing their molecular weight and enabling uniform dispersion of the emulsion, thereby making its application possible.

Next, for the sensitivity test, we prepared nuclear emulsion using each type of gelatin (crystal size of approximately 200 nm) and irradiated them with an electron beam at UVSOR. Figure 2 shows the micrographs of nuclear emulsions using each type of gelatin.

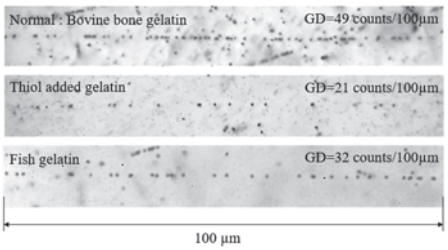

Fig.2. Micrographs of electron tracks recorded in nuclear emulsions with different gelatin compositions.

A sensitivity test was conducted as part of the development of nuclear emulsions with different types of gelatin. In the future, we plan to investigate the differences in sensitivity and the effects on latent image fading.

[1] K. Morishima *et al.*, Nature **552** (2017) 386.
[2] T. Tani *et al.*, Nucl. Instrum. Methods A **1006** (2021) 165427.

UVSOR User 8